Continuum Models of Carbon Nanotube-Based Composites Using the Boundary Element Method

Y.J. Liu and X.L. Chen
Department of Mechanical, Industrial and Nuclear Engineering
University of Cincinnati, P.O. Box 210072, Cincinnati, Ohio 45221-0072, U.S.A.
E-mail: Yijun.Liu@uc.edu

Abstract

This paper presents some recent advances in the boundary element method (BEM) for the analysis of carbon nanotube (CNT)-based composites. Carbon nanotubes, formed conceptually by rolling thin graphite sheets, have been found to be extremely stiff, strong and resilient, and therefore may be ideal for reinforcing composite materials. However, the thin cylindrical shape of the CNTs presents great challenges to any computational method when these thin shell-like CNTs are embedded in a matrix material. The BEM, based on exactly the same boundary integral equation (BIE) formulation developed by Rizzo some forty years ago, turns out to be an ideal numerical tool for such simulations using continuum mechanics. Modeling issues regarding model selections, representative volume elements, interface conditions and others, will be discussed in this paper. Methods for dealing with nearly-singular integrals which arise in the BEM analysis of thin or layered materials and are crucial for the accuracy of such analyses will be reviewed. Numerical examples using the BEM and compared with the finite element method (FEM) will be presented to demonstrate the efficiency and accuracy of the BEM in analyzing the CNT-reinforced composites.

1. Introduction

Ever since the seminal work by Professor Rizzo on elasticity [1] and other work that followed [2-8], BIE/BEM has been applied successfully to the analysis of various materials, such as anisotropic materials (see, e.g., [4, 7, 9-13]), composites [14-18] and piezoelectric materials [19-26]. There is a reason for this continued interest in the BIE/BEM for the analysis of various materials. Besides the often-cited advantage of the reduction in dimensions of the computational models, the BIE/BEM is superior in stress analysis, especially at the material interfaces, which are crucial to understanding the performance and integrity of materials. In recent years, the BEM has been found especially efficient in modeling many materials involving thin shell-like structures [27] or small features, such as composite materials with interphases (see, e.g., Refs. [28-30]), thin elastic films and coatings [31-33], thin piezoelectric films [34, 35], and the micro-electro-mechanical systems (MEMS) [36-40]. The efficiency in the solution of the BEM equations has also been improved dramatically in the last few years by the so-called fast multipole expansion methods (e.g., Refs. [41-43]).

Based on these distinctive features and the recent advances in improving its efficiency, the BIE/BEM approach will be a natural choice and may offer significant advantages in the analysis of carbon nanotube-based composites when the continuum

mechanics models are applicable. This paper will discuss the related issues in modeling CNT-based composites using continuum mechanics and present the first results in applying the BEM for such modeling to demonstrate the advantages of the BEM as compared with the domain-based FEM.

2. CNT-Based Composites and Modeling Considerations

Carbon nanotubes, discovered first by Iijima in 1991 [44], possess exceptionally high stiffness, strength and resilience, as well as superior electrical and thermal properties, which may become the ultimate reinforcing materials for the development of an entirely new class of composites (see, e.g., two recent reviews [45, 46]). It has been demonstrated that with just 1% (by weight) of CNTs added in a matrix, the stiffness of the resulting composite can increase between 36-42% and the tensile strength by 25% [47]. The mechanical-load carrying capacities of CNTs in nanocomposites have also been demonstrated in some experiments [47-50] and preliminary simulations [51, 52]. All these studies show the great potentials of CNT-based composites as well as the enormous challenges in the development of such nanocomposites. A comprehensive approach combining analytical, experimental and computational methods need to be adopted to tackle these multiscale, multiphysics problems in the development of nanocomposites [46].

Computational approaches can play a significant role in the development of nanocomposites. Modeling and simulations can help in the understanding, analysis and design of nanomaterials. At the nanoscale, analytical models are difficult to establish, while experiments are expensive to conduct. On the other hand, modeling of nanocomposites can be done effectively and efficiently. Some initial guidelines to the experimental work can be obtained readily by performing some modeling and simulation work to help reduce the scope, cost and time for the experiments. The main issues in simulations are the proper selection of the mathematical models or theories for the problems considered. Meaningful computer simulations are very much dependent on the accuracy of the mathematical models for the materials under investigation. For the continuum mechanics models in the study of mechanical properties of various materials, the two most commonly used numerical techniques have been the finite element method and boundary element method, both of which have the potential to play an important role in the modeling and simulations of nanomaterials.

Modeling materials at the nanoscale using the well established continuum mechanics approach is a new and challenging task for computational mechanics. Many of the modeling assumptions and approaches in the macro- and micro-mechanics may still be valid at the nanoscale when they are properly applied, while many others may not. Special considerations also arise from the unique geometry (thin shell-like structure) as well as the size of carbon nanotubes. Discussed below are just a few of the many considerations in modeling CNT-based nanocomposites, and many other issues will need to be addressed when the simulations develop into more sophisticated stages, involving, for example, multiphysics or defects.

(1) Can continuum models be applied to CNT-based composites?

The questions one has to answer first before conducting any simulations of

CNT-based composites are: What mathematical models should be applied to nanocomposites? Can continuum mechanics approach be applied safely to investigate nanocomposites? It is believed that the answers to these crucial questions depend largely on the purposes of the simulations. If the focus of the simulation is on *local* interactions among individual atoms, or chemical reactions between the CNT and a matrix material, then the mathematical models based on quantum mechanics or molecular dynamics (MD) should definitely be adopted. However, if the purpose of the simulation is to investigate the *global* responses of individual CNTs or CNT-based composites, such as deformations, load transfer mechanisms, or effective stiffness of the nanocomposites, then the continuum mechanics approach may still be applied safely to provide such information effectively and efficiently [45, 51-57].

Currently available main simulation models for carbon nanotubes can be categorized as discrete and continuum models (Fig. 1). The *discrete* models, such as molecular dynamics models, are applied widely in the nanoscale research. In these MD approaches, the atoms are considered as individual particles and the forces among them are calculated using potential theories. The equilibrium or dynamic equations for each particles are established for determining the displacement fields under given loads. These fundamental approaches have provided abundant simulation results for understanding the behaviors of individual or bundled CNTs [58-66]. However, these nanoscale simulations are currently limited to very small length and time scales and cannot deal with the larger length scales needed in characterizations of nanocomposites, due to the limitations of current computing power (e.g., a cube with an edge length of only 1 μm could contain up to 10^{12} atoms).
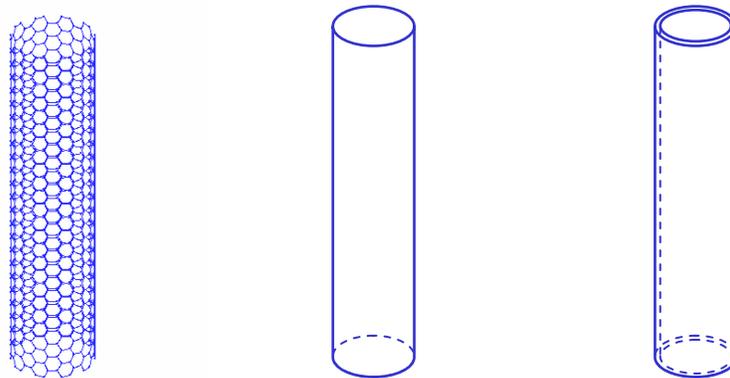
(a) Discrete (MD) model   (b) Continuum *shell* model   (c) Continuum *solid* model

Figure 1. Computational models of an individual carbon nanotube.

The *continuum mechanics* approach has also been applied successfully for simulating the mechanical responses of individual carbon nanotubes which are treated as beams, thin shells or solids in cylindrical shapes [53-55, 57, 67, 68]. The current results using the continuum approaches have indicated that continuum mechanics can be applied to models with dimensions of a few hundred nanometers and larger, where averaging of material properties can be done properly for CNTs. Although efficient in

computing and able to handle models at larger length scales, the continuum mechanics models at this threshold face the risk of breakdowns more than ever before, compared with the micromechanics simulations. Every effort should be made to ensure that the continuum assumptions are held and results are validated (with either experiments or other simulations). Simulation results obtained using the continuum mechanics approach should also be interpreted correctly. Attentions should be paid to overall deformations or load transfer mechanisms, rather than to local stresses, such as those at the interface between the CNTs and matrix, where the physics may need to be addressed by MD.

There are several options in the continuum mechanics approach for modeling the CNTs. *Beam* models are 1-D (line) models (usually straight) for slender structural members under bending loads. They have been applied successfully for calculating the overall responses of the CNTs, such as the deformation or vibration modes [53, 55]. *Shell* models, in which only the 2-D mid-surface of a thin structure is modeled, are easy in modeling and efficient in computing. In addition, CNTs are indeed thin shell-like, cylindrical structures. Several studies of the responses of individual CNTs using the shell models can be found in Refs. [57, 67, 68]. However, it is difficult to couple shell models with the 3-D solid model used for the matrix at the interfaces, since the two models involve different types of variables or degrees of freedom. It is therefore a natural and safe choice to apply the 3-D elasticity (solid) models for the analysis of CNTs when they are embedded in a matrix material. *Solid* models of the CNTs will provide the best possible accuracy among all the continuum mechanics models. One study of individual CNTs using the 3-D elasticity model can be found in Ref. [54]. Numerical methods, such as the finite element, boundary element and meshfree methods, can be applied readily for solving the 3-D multi-domain elasticity problems that describe the interactions of the CNTs and matrix, if careful attentions are given to the unique geometry of the CNTs.

Both the BEM and FEM will be employed in this paper to study the overall mechanical responses of the CNT-based composites. The advantages, disadvantages and potentials of each method in such simulations will be evident from these examples.

(2) Representative volume elements (RVE)

Carbon nanotubes are in different sizes and forms when they are dispersed in a matrix to form the nanocomposites. They can be single-walled or multi-walled with length of a few nanometers or a few micrometers, and can be straight, twisted and curled, or in the form of ropes [45-50]. Their orientation in the matrix can be unidirectional or random. All these factors make the simulations of the mechanical responses of nanotube-based materials extremely complicated. To start with, the concept of unit cells or representative volume elements, which have been applied successfully in the studies of conventional fiber-reinforced composites at the microscale [69, 70], can be extended to the study of CNT-based composites at the nanoscale. In this unit cell or RVE approach, a single nanotube with surrounding matrix material can be modeled, with properly applied boundary and interface conditions to account for the effects of the surrounding materials. This RVE model can be employed to study the interactions of the nanotube with the matrix, to investigate the load transfer mechanism, or to evaluate the effective material properties of the nanocomposite, as have been done

for conventional composites. However, since CNT fibers can be relatively short in length, 3-D RVEs may need to be applied for simulating CNT-based composites. The 2-D (plane strain) RVE or 1-D models for studying the responses in the transverse and axial directions of conventional composites, respectively, may not work for nanocomposites based on short CNTs. Requiring 3-D modeling of CNTs will make the simulations of nanocomposites even more demanding.

Three representative volume elements are proposed (Fig. 2) for the study of CNT-based composites. They are, according to the shape of the cross section, circular (cylindrical) RVE (Fig. 2 (a)), square RVE (Fig. 2 (b)) and hexagonal RVE (Fig. 2 (c)). The cylindrical RVE can be applied to model the cases when CNTs have different diameters [69]. Under axisymmetric loading, a 2-D (axisymmetric) analysis model can be applied for the cylindrical RVE, which can significantly reduce the computational work. Similar to the study of conventional fiber-reinforced composites [69], the square RVE models can be applied when the CNT fibers are arranged evenly in a square pattern, while the hexagonal RVE models can be applied when CNT fibers are in a hexagonal pattern, in the transverse directions. These RVEs can be used to provide the basic, whereas detailed, analyses of a CNT interacting with the matrix, such as the load transfer mechanism or stress distributions, without overwhelming the computing resources [51, 52].

With the increase of computing power and confidence in simulations of CNT-based composites, large-scale models containing more CNTs, distributed evenly or randomly, can be employed to investigate the interactions among CNTs in a matrix and to have a more accurate account of the characteristics of the CNT-based composites.
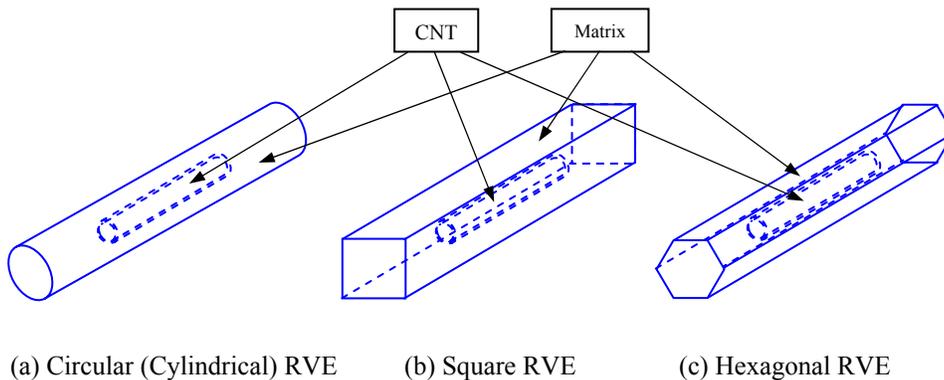

(a) Circular (Cylindrical) RVE   (b) Square RVE   (c) Hexagonal RVE

Figure 2. Three possible representative volume elements (RVE) for the analysis of CNT-based nanocomposites.

(3) Other considerations

Interfaces between the carbon nanotubes and matrix are crucial regions for the functionality and reliability of CNT-based nanocomposites. Whether or not the huge potentials of the CNTs as load carrying members can be realized in a nanocomposite depends almost entirely on whether or not strong interfaces can be achieved, since all the loads must be transferred through the interfaces to CNTs. Most failures of CNT-

based nanocomposites, like those of other composites, may occur at or around the interfaces, such as interface debonding, friction/wear, instability, or matrix cracking, because of the mismatch in the stiffness and other physical or chemical properties. From the modeling point of view, interfaces pose serious challenges to any simulation techniques based on the continuum mechanics. This is especially true at the nanoscale. At the nano or atomic scale, the interface is not even a continuous surface. Thus, simulations results near the interfaces should be interpreted carefully.

To start with, *perfect bonding* can be assumed between the CNTs and matrix in the modeling and simulation of nanocomposites using the continuum models. Research has demonstrated that the possibility of such a strong (C-C) bond exists for CNT-based composites [46, 71]. Other models, such as *spring-like* models (see, e.g., Ref. [15]) and a thin *interphase* models (see, e.g., Refs. [28-30]), can also be considered to model the interfaces between CNTs and the matrix.

Finally, an important issue in simulations of CNT-based composites using the continuum mechanics approach is how simulation results should be interpreted and utilized. Again, numerical results should be interpreted properly, considering the limitations of the continuum mechanics approach in such studies. For example, the deformation of an RVE or distribution and order of magnitude of stresses are more important to investigations of the load transfer mechanisms in a nanocomposite, than the actual maximum value and location of a certain stress component near the interfaces.

3. The BEM Formulation for CNT-Based Composites

For modeling CNT-based composites, the following conventional boundary integral equation for 3-D elastostatic problems [1, 8] can be applied:

$$\int_S T_{ij}(P,P_o)\big[u_j(P) - u_j(P_o)\big]dS(P) = \int_S U_{ij}(P,P_o)t_j(P)dS(P), \qquad \forall P_o \in S, \quad (1)$$

in which u_i and t_i are the displacement and traction fields, respectively; U_{ij} and T_{ij} the displacement and traction kernels, respectively; P the field point and P_o the source point; and S the boundary surface of the domain under consideration. Eq. (1) is a weakly-singular form of the conventional BIE and does not involve computations of any singular integrals in the discretization. This BIE can be applied safely to thin shell-like materials or structures, as long as the nearly-singular integrals can be computed accurately and efficiently [27, 31].

In the current study of the CNT-based composites, BIE (1) is applied in each domain of the CNT and the matrix separately. The resulting two equations from the two domains are coupled at the interfaces of the CNT and the matrix. Perfect bonding conditions are assumed, that is, continuity of the displacement fields and equilibrium of the tractions are enforced at the interface.

The key step in a successful application of the BEM to the analysis of CNT-based composites is to compute nearly-singular integrals accurately. Nearly-singular integrals occur when the source point is very close to but still off the surface of integration. For example, the integration may be on the outer surface of a CNT (a thin

cylindrical shell in the continuum model), while the source point is located on the inner surface of the CNT. Although other methods such as subdivisions can be applied to deal with these nearly-singular integrals, the most efficient and accurate one is believed to be the line-integral approach [27, 72]. For example, the integral with the traction kernel on a surface ΔS with the source point P_0 nearby can be isolated and further transformed into line integrals using the Stokes' theorem as follows [27, 72]:

$$\int_{\Delta S} T_{ij}(P,P_o)dS(P) = I_\Omega(P_0) + \frac{1}{4\pi}\varepsilon_{ijk}\oint_C\frac{1}{r}dx_k + \frac{1}{8\pi(1-\nu)}\varepsilon_{jkl}\oint_C r_{,ik}dx_l \qquad (2)$$

in which C is the boundary curve of ΔS, r the distance between P_0 and P, ν the Poisson's ratio, and ε_{ijk} the permutation tensor. The first term on the right-hand side of Eq. (2) is a solid angle integral:

$$I_\Omega(P_0) = \int_{\Delta S}\frac{\partial G}{\partial n}dS = -\frac{1}{4\pi}\int_{\Delta S}\frac{1}{r^2}\frac{\partial r}{\partial n}dS \qquad (3)$$

where $G = 1/4\pi r$ is the Green's function for 3-D potential problems. This solid angle integral (a surface integral) can be transformed into a line integral on the bounding curve C as well [27]:

$$I_\Omega(P_0) = \frac{1}{4\pi}\oint_C\left[\frac{Z(L)}{R(L)} - 1\right]\frac{(\hat{\rho}\cdot\hat{v})(\hat{t}\cdot\hat{\eta})}{\rho}dL \qquad (4)$$

in which the variables R, Z, ρ, $\hat{\rho}$, $\hat{v}$, $\hat{t}$ and $\hat{\eta}$ are some geometric-related parameters defined on the boundary curve C or its projection to a coordinate plane [27].

It does require some efforts to implement the line integral approach using Eqs. (2) and (4) for dealing with nearly-singular integrals in a 3-D BEM code, which in general only deals with singular and non-singular integrals. A straightforward approach to dealing with nearly-singular integrals in a BEM code is often to consider them as nonsingular integrals and apply smaller elements or subdivide elements into smaller cells. This has been the approach adopted by many BEM code and has been shown to be inefficient. Extra effort in implementing the line integral approach (Eqs. (2) and (4)) in a structural BEM code will not slow down the code at all when thin bodies need to be considered, since the line integrals are much faster to compute and much easier to compute accurately than the corresponding area integrals.

The line-integral approach to dealing with the nearly-singular integrals containing the traction kernel has been shown to be very successful in analyzing 3-D shell-like structures and open crack problems [27, 73]. This approach has also been implemented for the 2-D elasticity cases with further improvement for integrals with weak singularities [31-33]. The extension to deal with 2-D piezoelectric BIE has also been carried out in Ref. [35].

Further improvements for dealing with the nearly-singular integrals in the 3-D case has been done recently by employing a nonlinear coordinate transformation for the integrals with the displacement kernel and the regularized integrals with the traction kernel, both can be nearly-weakly singular for a thin body or thin shape, as discussed in

[31] in the 2-D cases. Detailed implementation of this nonlinear transformation for 3-D problems and improved numerical test results will be presented in Ref. [74]. With these improvements, the source point can be placed closer to the element of integration without the need to subdivide the element. The line-integral approach and the improvements mentioned above are all employed in this study for analyzing the CNT-based composites, where the CNT thickness can be extremely small compared with its other dimensions.

4. Numerical Examples

To demonstrate the difficulties in the modeling of CNT-based nanocomposites and the advantages of the BEM over the FEM in such modeling, a short single-walled carbon nanotube embedded in a matrix material is studied using a square RVE (Fig. 3). The advanced multi-domain BEM based on the work in Refs. [27, 74] is applied to the square RVE model. The commercial package ANSYS is used for the FEM modeling.
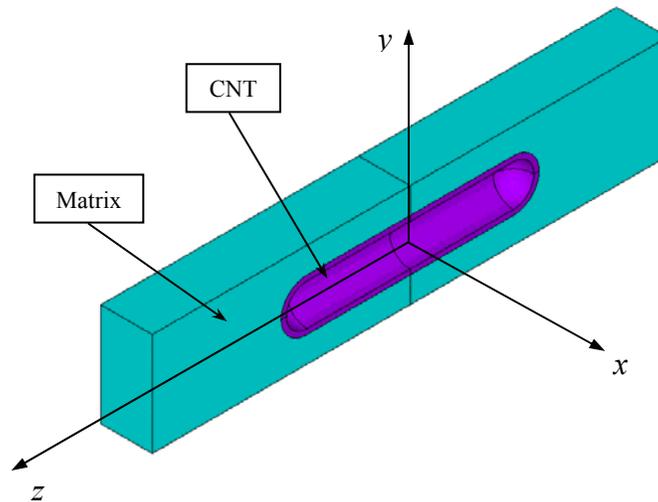

Figure 3. A square RVE shown in a cut-through view.

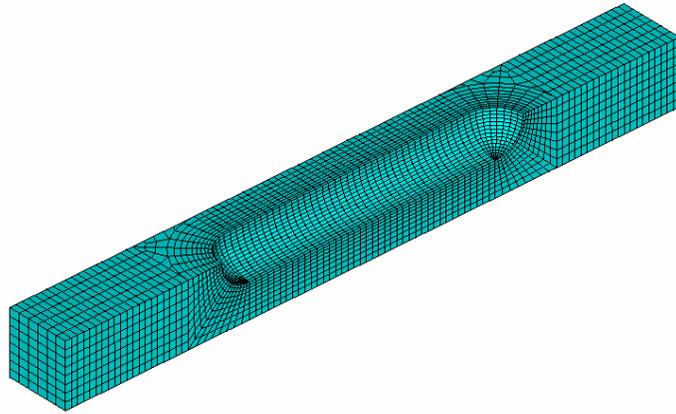The dimensions used for the full square RVE are:
Matrix: height = width = 10 nm, length = 100 nm;
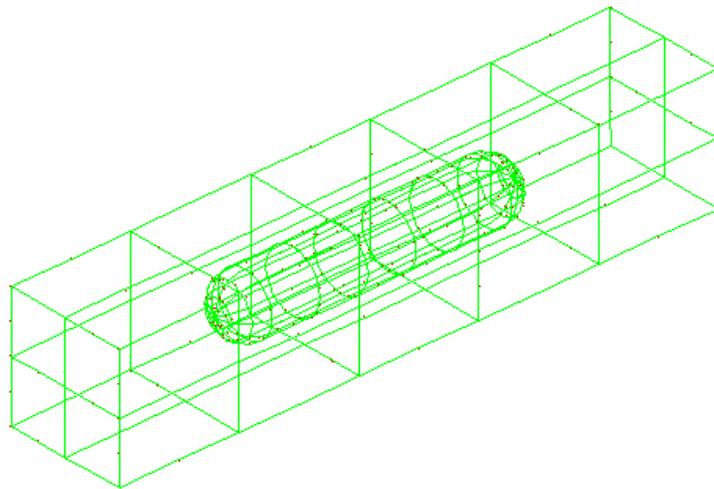CNT: outer radius = 5 nm, inner radius r_i =4.6 nm, length = 50 nm.

The Young's moduli and Poisson's ratios are:
Matrix: $E_m = 100\,\text{nN/nm}^2\ (= 100\,\text{GPa}),\ \nu_m = 0.3$;
CNT: $E_{CNT} = 1000\,\text{nN/nm}^2\ (= 1000\,\text{GPa}),\ \nu_{CNT} = 0.3$.

(a) An FEM mesh (quarter model, 10,240 quadratic solid elements)

(b) A BEM mesh (full model, 312 quadratic surface elements)

Figure 4. Comparison of the FEM and BEM discretizations for a square RVE
(CNT thickness = 0.4 nm).

The effective thickness of the CNT used is 0.4 nm (the theoretical value of the thickness of a single-walled CNT is approximately 0.34 nm [45]). These values for the dimensions of the CNT and material constants are chosen within the wide ranges of those for CNTs as reported in the literature [53, 61, 64, 65, 75-81] and can be adjusted readily for a specific case in future simulations. For the interface conditions, perfect bonding between the CNT and matrix is assumed in all the cases studied.

An FEM mesh with converged results for a quarter symmetry model of the RVE is shown in Fig. 4 (a) and a BEM mesh for the full model is shown in Fig. 4 (b). For the FEM model, quadratic brick elements are employed and one layer of elements are used through the thickness of the CNT. Elements with small sizes are needed also in the matrix near the CNT, due to the element connectivity and aspect ratio restrictions in the FEM. Thus, a large number of finite elements (10,240 in total) are needed in this quarter-symmetric FEM model for this analysis.

On the other hand, in the full BEM model shown in Fig. 4 (b), a very small number of quadratic surface elements (312 in total) are employed on the interface and boundaries only (the cylindrical CNT is represented by the inner and outer surfaces in the BEM model). The element sizes in the BEM models can be independent of the CNT thickness, because the advanced 3-D multi-domain BEM can handle the thin shell-like CNT domain very effectively and accurately without the need to increase the number of elements (see Refs. [27] for more details).

As the first loading case to study the overall deformation of the RVE, a bending load is applied to the square RVE, which is fixed at both ends and applied with a distributed load q (in the negative y direction, Fig. 3) on both the top and bottom surfaces (such that an FEM quarter model can be applied for this antisymmetric case). The contour plots for the deformed shapes of the square RVE using the FEM and BEM are shown in Fig. 5 (a) and Fig. 5 (b), respectively. The difference between the FEM and BEM results for the deformation is less than 5% (Table 1).

As the second loading case to study the load transfer mechanism of the RVE for CNT-based composites, an axial stretch ΔL is applied to the RVE along the CNT direction at one end and the displacement is fixed at the other end. The contour plots for the stress distributions using the FEM and BEM are shown in Fig. 6 (a) and Fig. 6 (b), respectively. The load carrying capacity of the CNT can be observed from these plots, as the high stresses (represented by red color) are confined mostly within or near the CNT. With larger ratios of the CNT Young's modulus to that of the matrix (i.e., E_{CNT}/E_m, which is 10 in the current case), or long CNTs, the load carrying capacities of the CNTs will be even more prominent (more examples using the FEM can be found in Ref. [51, 52]). The stress results using the FEM and BEM are almost identical as shown in Fig. (6) and the advantages of the BEM in the modeling of the CNT-based composites are obvious (Table 2) regarding the meshing (volumes versus surfaces) and number of elements applied.
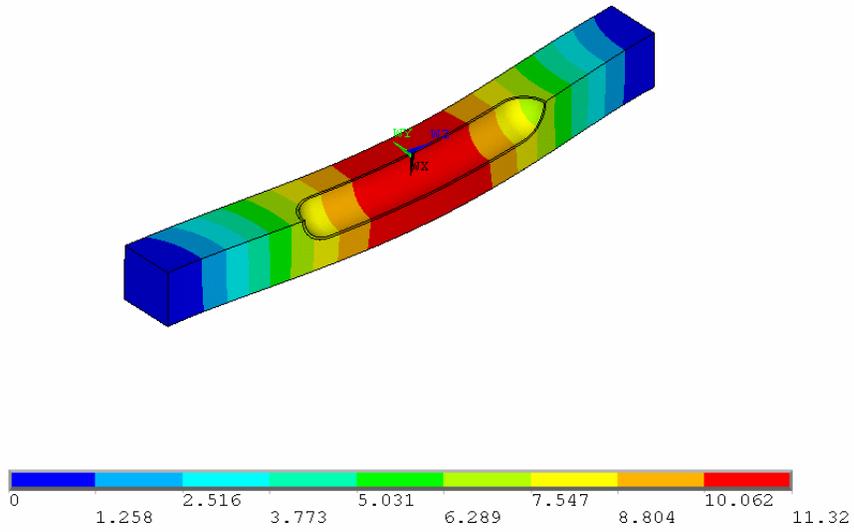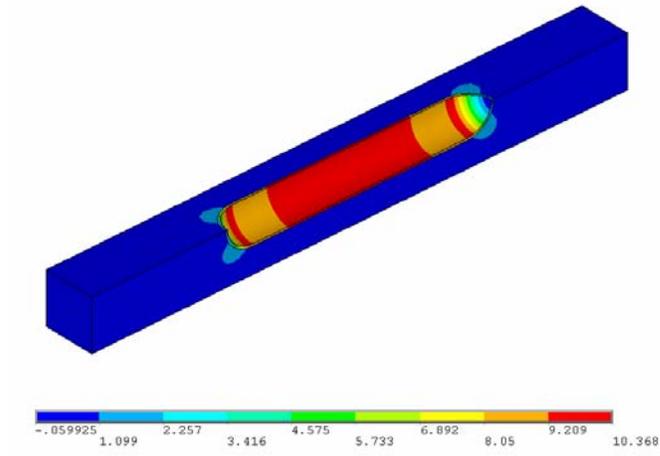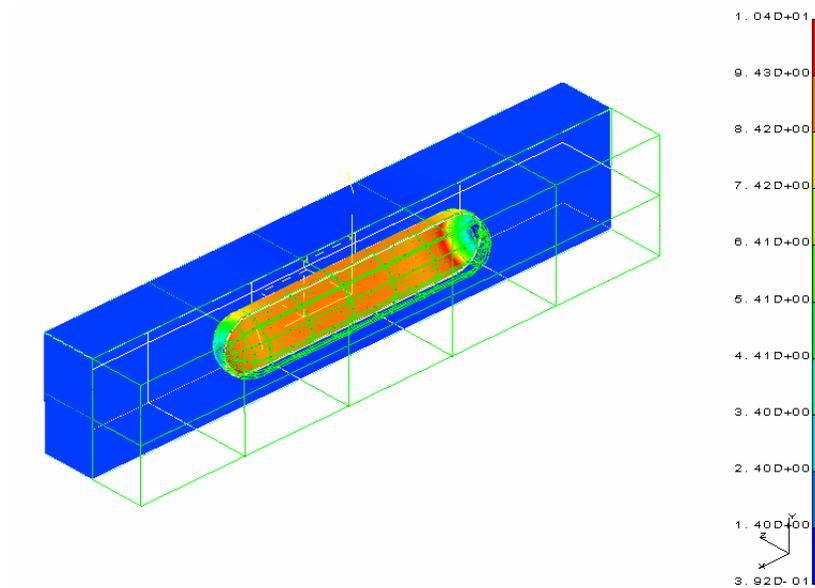
(a) FEM result ($\times q$; quarter model)
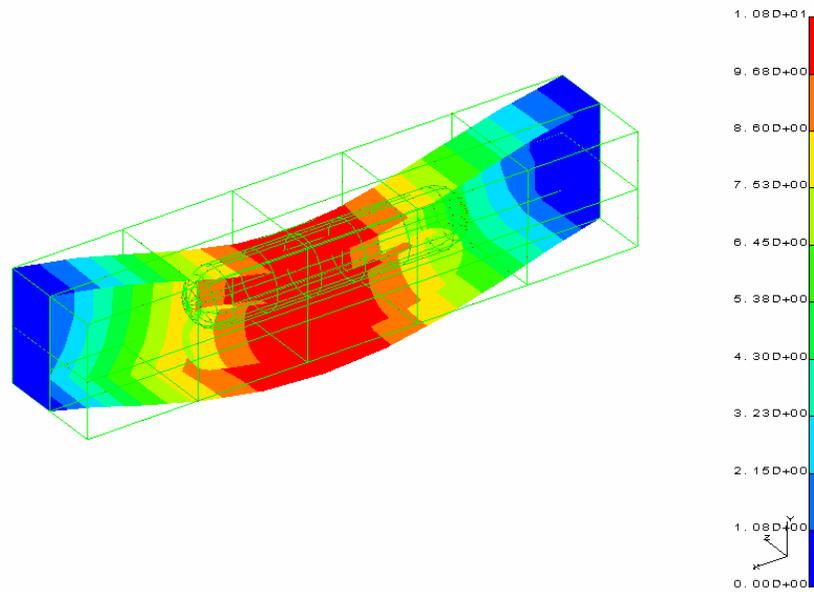
(b) BEM result ($\times q$; full model in a cut-through view)

Figure 5. Deformed shapes of the square RVE under a bending load q.

(a)   FEM result ($\times \Delta L$; quarter model)

(b) BEM result ($\times \Delta L$; full model in a cut-through view of the CNT only)

Figure 6. Stress distributions in the square RVE under an axial stretch ΔL .

Table 1. Comparison of the maximum displacement of the RVE under the bending load

	BEM (Full Model)	FEM (Quarter Model)
Number of elements	312	10,240
Max displacement (x q)	10.80	11.32

Table 2. Comparison of the maximum von Mises stress in the RVE under the stretch

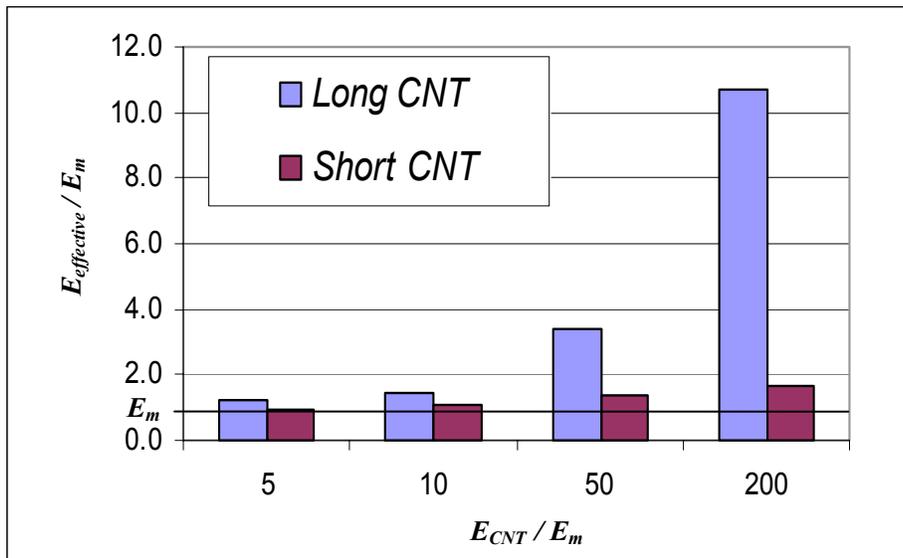|	BEM (Full Model)	FEM (Quarter Model)
Number of elements	312	10,240
Max von Mises stress (x ΔL)	10.40	10.37

Figure 7. Effective Young's moduli in the CNT direction for CNT modulus = 1,000 GPa, thickness = 0.4 nm, volume fraction = 0.05 (long) and 0.02 (short) ([51]).

The examples presented in this section are preliminary and aimed to study the feasibilities of characterizing CNT-based composites using the BEM and FEM based on the 3-D RVEs proposed. The main goal of using the BEM or FEM models of the RVEs is to help determine the effective material properties of the CNT-based composites. For this purpose, the overall deformations of the RVEs under different loadings need to be investigated and the continuum models are most likely applicable. Examples of evaluating the effective material constants of the CNT-based composites using the FEM models of the RVEs can be found in Refs. [51, 52]. A plot of the computed effective Young's moduli based on the data using the RVEs is given in Fig. 7, where increases of the effective Young's modulus in the CNT composites are plotted versus the Young's modulus ratios of the CNT and matrix. As can be seen from Figure 7, the reinforcing effects of the CNTs in the stiffness of a CNT-based composite is significant with a small volume fraction of the CNT (2 ~ 5 %), especially for cases with long CNTs and CNTs placed in a "soft" matrix (in Figure 7, $E_{CNT}/E_m = 200$ is corresponding to the case of a polymer matrix with CNT fibers, while $E_{CNT}/E_m = 5$ to the case of a steel matrix with CNT fibers) [51, 52]. More realistic models, for example, multi-walled CNTs, CNTs of large aspect ratios, and larger RVEs containing hundreds of CNTs with random distributions, can certainly be attempted in further investigations using the BEM, where the FEM modeling (meshing) will be even more difficult.

5. Discussions

The BIE/BEM has been applied successfully to analyzing many material related problems for the last four decades. However, applications of the BEM to analyzing thin and layered materials in particular or shell-like structures in general have long been regarded as, at least, an unwise exercise. This is due to the common belief that the BIE/BEM is not suitable for shell-like problems because degeneracy of the conventional BIE will arise as in the case of the BIE for crack problems. This belief, however, was challenged recently and it can be shown now [27, 82] that the conventional BIE for elasticity will give two distinctive equations across the thickness of a thin shell with vanishing thickness. Thus, the well-known elasticity BIE [1] will not degenerate for a well-posed elasticity problem and can be applied safely to shell-like structures, as long as the nearly-singular integrals can be computed accurately. The hypersingular (traction) BIE is not needed for analyzing shell-like structures, contrary to crack problems. This has opened up a wide area of applications for the BEM in the modeling and simulations of various materials involving thin interface regions, thin films or coatings, or layered materials. The application of the BEM to modeling CNT-based composites, reported in this paper, is just another example of how the BEM can be applied to tackle even the most challenging and urgent material modeling problems. This can be done by using exactly the same BIE developed by Rizzo some forty years ago [1], as long as the continuum mechanics assumptions are still valid and the simulation results are interpreted correctly.

Various considerations in the modeling of CNT-based composites using the continuum mechanics approach for the purpose of characterizations are discussed in this paper. Three representative volume elements, which are extensions of those used in

studying conventional composites, are proposed for the study of a CNT-based composites. 3-D elasticity models are proposed for modeling the cylindrical, thin shell-like CNTs when they are embedded in a matrix material. Methods for dealing with the nearly-singular integrals in the BEM arising in this case are reviewed. Numerical examples presented in this paper show that modeling and simulations of CNTs in a matrix can be very demanding even for the continuum mechanics approach. In general, detailed 3-D models with very fine meshes are needed for the FEM in order to obtain converged results. The BEM can use much fewer surface elements in this modeling and thus offers some clear advantages over the FEM.

There are still many challenges before the BEM can be a practical numerical tool for the analysis of CNT-based composites. For example, to model a large number of CNTs in a matrix, new approaches based on the BEM or its new variations (e.g., the boundary-node method [83, 84]) need to be developed. To improve the efficiency of the BEM, the use of the fast multipole expansion BEM [41-43] is inevitable. Finally, multiscale approaches that can link models at the nano, micro and macro scales need to be developed using a combination of two or three numerical methods aimed at different scales. There is much to do in the modeling and simulation of CNT-based composites and other nanomaterials. The BEM will contribute to this emerging field of material research with its unique features, just like it has done since the 1960's for the development of other materials.

Acknowledgments

References

1. F. J. Rizzo, "An integral equation approach to boundary value problems of classical elastostatics," *Quart. Appl. Math.*, **25**, 83-95 (1967).

2. T. A. Cruse and F. J. Rizzo, "A direct formulation and numerical solution of the general transient elastodynamic problem - I," *J. Math. Anal. & Appl.*, **22**, 244-259 (1968).

3. F. J. Rizzo and D. J. Shippy, "A formulation and solution procedure for the general non-homogeneous elastic inclusion problem," *Int. J. of Solids & Structures*, **4**, 1161-1179 (1968).

4. F. J. Rizzo and D. J. Shippy, "A method for stress determination in plane anisotropic elastic bodies," *J. Composite Materials*, **4**, 36-61 (1970).

5. F. J. Rizzo and D. J. Shippy, "A method of solution for certain problems of transient heat conduction," *AIAA J.*, **8**, 2004-2009 (1970).

6. F. J. Rizzo and D. J. Shippy, "An application of the correspondence principle of linear viscoelasticity theory," *SIAM J. Appl. Math.*, **21**, 321-330 (1971).

7. S. M. Vogel and F. J. Rizzo, "An integral equation formulation of three-dimensional anisotropic elastostatic boundary value problems," *J. Elasticity*, **3**,

203-216 (1973).

8. F. J. Rizzo and D. J. Shippy, "An advanced boundary integral equation method for three-dimensional thermoelasticity," *Int. J. Numer. Methods Engrg.*, **11**, 1753-1768 (1977).

9. R. B. Wilson and T. A. Cruse, "Efficient implementation of anisotropic three dimensional boundary-integral equation stress analysis," *Int. J. Numer. Methods Engrg.*, **12**, 1383-1397 (1978).

10. N. A. Schclar, *Anisotropic Analysis Using Boundary Elements* (Computational Mechanics Publications, Southampton, UK, 1994).

11. M. M. Perez and L. C. Wrobel, "An integral-equation formulation for anisotropic elastostatics," *J. Appl. Mech.*, **63**, 891-902 (1996).

12. J. R. Berger and V. K. Tewary, "Boundary integral equation formulation for interface cracks in anisotropic materials," *Comput. Mech.*, **20**, 261-266 (1997).

13. M. A. Sales and L. J. Gray, "Evaluation of the anisotropic Green's function and its derivatives," *Comput. & Struct.*, **69**, 247-254 (1998).

14. J. Mackerle, "Finite element and boundary element library for composites - a bibliography (1991-1993)," *Finite Elements in Analysis and Design*, **17**, 155-165 (1994).

15. J. D. Achenbach and H. Zhu, "Effect of interfacial zone on mechanical behavior and failure of fiber-reinforced composites," *J. Mech. Phys. Solids*, **37**, 381-393 (1989).

16. H. Zhu and J. D. Achenbach, "Effect of fiber-matrix interphase defects on microlevel stress states at neighboring fibers," *J. Composite Materials*, **25**, 224-238 (1991).

17. S. N. Gulrajani and S. Mukherjee, "Sensitivities and optimal design of hexagonal array fiber composites with respect to interphase properties," *Int. J. of Solids & Structures*, **30**, 2009-2026 (1993).

18. L. Pan, D. O. Adams, and F. J. Rizzo, "Boundary element analysis for composite materials and a library of Green's functions," *Comput. & Struct.*, **66**, 685-693 (1998).

19. J. S. Lee and L. Z. Jiang, "A boundary integral formulation and 2D fundamental solution for piezoelastic media," *Mech. Res. Comm.*, **21**, 47-54 (1994).

20. T. Chen and F. Z. Lin, "Boundary integral formulations for three-dimensional anisotropic piezoelectric solids," *Comput. Mech.*, **15**, 485-496 (1995).

21. J. S. Lee, "Boundary element method for electroelastic interaction in piezoceramics," *Engrg. Anal. Boundary Elements*, **15**, 321-328 (1995).

22. H. Ding, G. Wang, and W. Chen, "A boundary integral formulation and 2D fundamental solutions for piezoelectric media," *Comput. Methods Appl. Mech. Engrg.*, **158**, 65-80 (1998).

23. L. R. Hill and T. N. Farris, "Three-dimensional piezoelectric boundary element method," *AIAA J.*, **36**, 102-108 (1998).

24. X.-L. Xu and R. K. N. D. Rajapakse, "Boundary element analysis of piezoelectric

solids with defects," *Composites Part B - Engineering*, **29**, 655-669 (1998).

25. E. Pan, "A BEM analysis of fracture mechanics in 2D anisotropic piezoelectric solids," *Engrg. Anal. Boundary Elements*, **23**, 67-76 (1999).

26. M. Kogl and L. Gaul, "A boundary element method for transient piezoelectric analysis," *Engrg. Anal. Boundary Elements*, **24**, 591-598 (2000).

27. Y. J. Liu, "Analysis of shell-like structures by the boundary element method based on 3-D elasticity: formulation and verification," *Int. J. Numer. Methods Engrg.*, **41**, 541-558 (1998).

28. Y. J. Liu, N. Xu, and J. F. Luo, "Modeling of interphases in fiber-reinforced composites under transverse loading using the boundary element method," *J. Appl. Mech.*, **67**, 41-49 (2000).

29. Y. J. Liu and N. Xu, "Modeling of interface cracks in fiber-reinforced composites with the presence of interphases using the boundary element method," *Mechanics of Materials*, **32**, 769-783 (2000).

30. X. L. Chen and Y. J. Liu, "Multiple-cell modeling of fiber-reinforced composites with the presence of interphases using the boundary element method," *Computational Materials Science*, **21**, 86-94 (2001).

31. J. F. Luo, Y. J. Liu, and E. J. Berger, "Analysis of two-dimensional thin structures (from micro- to nano-scales) using the boundary element method," *Comput. Mech.*, **22**, 404-412 (1998).

32. J. F. Luo, Y. J. Liu, and E. J. Berger, "Interfacial stress analysis for multi-coating systems using an advanced boundary element method," *Comput. Mech.*, **24**, 448-455 (2000).

33. X. L. Chen and Y. J. Liu, "Thermal stress analysis of multi-layer thin films and coatings by an advanced boundary element method," *CMES: Computer Modeling in Engineering & Sciences*, **2**, 337-350 (2001).

34. Y. J. Liu and H. Fan, "On the conventional boundary integral equation formulation for piezoelectric solids with defects or of thin shapes," *Engrg. Anal. Boundary Elements*, **25**, 77-91 (2001).

35. Y. J. Liu and H. Fan, "Analysis of thin piezoelectric solids by the boundary element method," *Comput. Methods Appl. Mech. Engrg.*, **191**, 2297-2315 (2002).

36. F. Shi, P. Ramesh, and S. Mukherjee, "Simulation methods for micro-electro-mechanical structures (MEMS) with application to a microtweezer," *Comput. & Struct.*, **56**, 769-783 (1995).

37. F. Shi, P. Ramesh, and S. Mukherjee, "Dynamic analysis of micro-electro-mechanical systems (MEMS)," *Int. J. Numer. Methods Engrg.*, **39**, 4119-4139 (1996).

38. W. Ye and S. Mukherjee, "Optimal shape design of three-dimensional MEMS with applications to electrostatic comb drives," *Int. J. Numer. Methods Engrg.*, **45**, 175-194 (1999).

39. W. Ye and S. Mukherjee, "Design and fabrication of an electrostatic variable gap comb drive in micro-electro-mechanical systems," *CMES: Computer Modeling in*

Engineering & Sciences, **1**, 111-120 (2000).

40. P. Ljung, M. Bachtold, and M. Spasojevic, "Analysis of realistic large MEMS devices," *CMES: Computer Modeling in Engineering & Sciences*, **1**, 21-30 (2000).

41. J. E. Gomez and H. Power, "A multipole direct and indirect BEM for 2D cavity flow at low Reynolds number," *Engrg. Anal. Boundary Elements*, **19**, 17-31 (1997).

42. Y. Fu, K. J. Klimkowski, G. J. Rodin, E. Berger, J. C. Browne, J. K. Singer, R. A. V. D. Geijn, and K. S. Vemaganti, "A fast solution method for three-dimensional many-particle problems of linear elasticity," *Int. J. Numer. Methods Engrg.*, **42**, 1215-1229 (1998).

43. N. Nishimura, K.-i. Yoshida, and S. Kobayashi, "A fast multipole boundary integral equation method for crack problems in 3D," *Engrg. Anal. Boundary Elements*, **23**, 97-105 (1999).

44. S. Iijima, "Helical microtubules of graphitic carbon," *Nature*, **354**, 56–58 (1991).

45. D. Qian, G. J. Wagner, W. K. Liu, M.-F. Yu, and R. S. Ruoff, "Mechanics of carbon nanotubes," *Appl. Mech. Rev.*, **55**, 495-533 (2002).

46. E. T. Thostenson, Z. F. Ren, and T.-W. Chou, "Advances in the science and technology of carbon nanotubes and their composites: a review," *Composites Science and Technology*, **61**, 1899-1912 (2001).

47. D. Qian, E. C. Dickey, R. Andrews, and T. Rantell, "Load transfer and deformation mechanisms in carbon nanotube-polystyrene composites," *Applied Physics Letters*, **76**, 2868-2870 (2000).

48. H. D. Wagner, O. Lourie, Y. Feldman, and R. Tenne, "Stress-induced fragmentation of multiwall carbon nanotubes in a polymer matrix," *Applied Physics Letters*, **72**, 188-190 (1998).

49. L. S. Schadler, S. C. Giannaris, and P. M. Ajayan, "Load transfer in carbon nanotube epoxy composites," *Applied Physics Letters*, **73**, 3842-3844 (1998).

50. C. Bower, R. Rosen, L. Jin, J. Han, and O. Zhou, "Deformation of carbon nanotubes in nanotube-polymer composites," *Applied Physics Letters*, **74**, 3317-3319 (1999).

51. Y. J. Liu and X. L. Chen, "Evaluations of the effective materials properties of carbon nanotube-based composites using a nanoscale representative volume element," *Mechanics of Materials*, **35**, 69-81 (2003).

52. X. L. Chen and Y. J. Liu, "Square representative volume elements for evaluating the effective material properties of carbon nanotube-based composites," *Computational Materials Science*, in press (2003).

53. E. W. Wong, P. E. Sheehan, and C. M. Lieber, "Nanobeam mechanics: Elasticity, strength, and toughness of nanorods and nanotubes," *Science*, **277**, 1971-1975 (1997).

54. K. Sohlberg, B. G. Sumpter, R. E. Tuzun, and D. W. Noid, "Continuum methods of mechanics as a simplified approach to structural engineering of

nanostructures," *Nanotechnology*, **9**, 30-36 (1998).

55. S. Govindjee and J. L. Sackman, "On the use of continuum mechanics to estimate the properties of nanotubes," *Solid State Communications*, **110**, 227-230 (1999).

56. C. Q. Ru, "Elastic buckling of single-walled carbon nanotube ropes under high pressure," *Physical Review B*, **62**, 10405-10408 (2000).

57. C. Q. Ru, "Axially compressed buckling of a doublewalled carbon nanotube embedded in an elastic medium," *J. Mech. Phys. Solids*, **49**, 1265-1279 (2001).

58. D. Srivastava, M. Menon, and K. Cho, "Computational Nanotechnology with Carbon Nanotubes and Fullerenes," *Computing in Science and Engineering*, **3**, 42-55 (2001).

59. M. Macucci, G. Iannaccone, J. Greer, J. Martorell, D. W. L. Sprung, A. Schenk, I. I. Yakimenko, K.-F. Berggren, K. Stokbro, and N. Gippius, "Status and perspectives of nanoscale device modelling," *Nanotechnology*, **12**, 136-142 (2001).

60. J. Han, A. Globus, R. Jaffe, and G. Deardorff, "Molecular dynamics simulations of carbon nanotube-based gears," *Nanotechnology*, **8**, 95-102 (1997).

61. C. F. Cornwell and L. T. Wille, "Elastic properties of single-walled carbon nanotubes in compression," *Solid State Communications*, **101**, 555-558 (1997).

62. S. B. Sinnott, O. A. Shenderova, C. T. White, and D. W. Brenner, "Mechanical properties of nanotubule fibers and composites determined from theoretical calculations and simulations," *Carbon*, **36**, 1-9 (1998).

63. T. Halicioglu, "Stress calculations for carbon nanotubes," *Thin Solid Films*, **312**, 11-14 (1998).

64. G. H. Gao, T. Cagin, and W. A. Goddard, "Energetics, structure, mechanical and vibrational properties of single-walled carbon nanotubes," *Nanotechnology*, **9**, 184-191 (1998).

65. M. Buongiorno Nardelli, J.-L. Fattebert, D. Orlikowski, C. Roland, Q. Zhao, and J. Bernholc, "Mechanical properties, defects and electronic behavior of carbon nanotubes," *Carbon*, **38**, 1703-1711 (2000).

66. J.-W. Kang and H.-J. Hwang, "Mechanical deformation study of copper nanowire using atomistic simulation," *Nanotechnology*, **12**, 295-300 (2001).

67. C. Q. Ru, "Column buckling of multiwalled carbon nanotubes with interlayer radial displacements," *Physical Review B*, **62**, 16962-16967 (2000).

68. D. Qian, W. K. Liu, and R. S. Ruoff, "Mechanics of C_{60} in nanotubes," *J. Phys. Chem. B*, **105**, 10753-10758 (2001).

69. M. W. Hyer, *Stress Analysis of Fiber-Reinforced Composite Materials*, 1st ed (McGraw-Hill, Boston, 1998).

70. S. Nemat-Nasser and M. Hori, *Micromechanics: Overall Properties of Heterogeneous Materials*, 2nd rev. ed (Elsevier, Amsterdam, 1999).

71. Z. Jia, Z. Wang, C. Xu, J. Liang, B. Wei, D. Wu, and S. Zhu, "Study on poly(methyl methacrylate)/carbon nanotube composites," *Materials Science and Engineering: A*, **271**, 395 - 400 (1999).

72. Y. J. Liu, D. M. Zhang, and F. J. Rizzo, "Nearly singular and hypersingular integrals in the boundary element method", in: eds. C. A. Brebbia and J. J. Rencis, Boundary Elements XV (Computational Mechanics Publications, Worcester, MA, 1993) 453-468.

73. Y. J. Liu and F. J. Rizzo, "Scattering of elastic waves from thin shapes in three dimensions using the composite boundary integral equation formulation," *J. Acoust. Soc. Am.*, **102 (2)**, 926-932 (1997).

74. X. L. Chen and Y. J. Liu, "Analysis of 3-D thin layered structures by an advanced boundary element method," in preparation (2003).

75. R. S. Ruoff and D. C. Lorents, "Mechanical and thermal properties of carbon nanotubes," *Carbon*, **33**, 925-930 (1995).

76. M. M. J. Treacy, T. W. Ebbesen, and J. M. Gibson, "Exceptionally high Young's modulus observed for individual carbon nanotubes," *Nature*, **381**, 678-680 (1996).

77. J. P. Lu, "Elastic properties of single and multilayered nanotubes," *Journal of Physics and Chemistry of Solids*, **58**, 1649-1652 (1997).

78. A. Krishnan, E. Dujardin, T. W. Ebbesen, P. N. Yianilos, and M. M. J. Treacy, "Young's modulus of single-walled nanotubes," *Physical Review B-Condensed Matter*, **58**, 14013-14019 (1998).

79. N. Yao and V. Lordi, "Young's modulus of single-walled carbon nanotubes," *Journal of Applied Physics*, **84**, 1939-1943 (1998).

80. C. Goze, P. Bernier, L. Henrard, L. Vaccarini, E. Hernandez, and A. Rubio, "Elastic and mechanical properties of carbon nanotubes," *Synthetic Metals*, **103**, 2500-2501 (1999).

81. J. P. Salvetat, J. M. Bonard, N. H. Thomson, A. J. Kulik, L. Forro, W. Benoit, and L. Zuppiroli, "Mechanical properties of carbon nanotubes," *Applied Physics A - Materials Science & Processing*, **69**, 255-260 (1999).

82. S. Mukherjee, "On boundary integral equations for cracked and for thin bodies," *Mathematics and Mechanics of Solids*, **6**, 47-64 (2001).

83. Y. X. Mukherjee and S. Mukherjee, "The boundary node method for potential problems," *Int. J. Numer. Methods Engrg.*, **40**, 797-815 (1997).

84. M. K. Chati, S. Mukherjee, and Y. X. Mukherjee, "The boundary node method for three-dimensional linear elasticity," *Int. J. Numer. Methods Engrg.*, **46**, 1163-1184 (1999).